Bmi1 Functions as an Oncogene Independent of Ink4A/Arf Repression in Hepatic Carcinogenesis

Chuan-Rui Xu,[1,3,4] Susie Lee,[1] Coral Ho,[1] Prashant Bommi,[5] Shi-Ang Huang,[3] Siu Tim Cheung,[7] Goberdhan P. Dimri,[5,6] and Xin Chen[1,2]

[1]Department of Bioengineering and Therapeutic Sciences and [2]Liver Center, University of California, San Francisco, California; [3]Center for Stem Cell Research and Application, Union Hospital and [4]School of Pharmacy of Huazhong University of Science and Technology, Wuhan, P.R. of China; [5]Department of Medicine, NorthShore University Health System Research Institute, Evanston, Illinois; [6]The Robert H. Lurie Comprehensive Cancer Center, Feinberg School of Medicine, Northwestern University, Chicago, Illinois; and [7]Department of Surgery, The University of Hong Kong, Hong Kong, China

Abstract

Bmi1 is a polycomb group proto-oncogene that has been implicated in multiple tumor types. However, its role in hepatocellular carcinoma (HCC) development has not been well studied. In this article, we report that Bmi1 is overexpressed in human HCC samples. When Bmi1 expression is knocked down in human HCC cell lines, it significantly inhibits cell proliferation and perturbs cell cycle regulation. To investigate the role of Bmi1 in promoting liver cancer development *in vivo*, we stably expressed Bmi1 and/or an activated form of Ras (RasV12) in mouse liver. We found that while Bmi1 or RasV12 alone is not sufficient to promote liver cancer development, coexpression of Bmi1 and RasV12 promotes HCC formation in mice. Tumors induced by Bmi1/RasV12 resemble human HCC by deregulation of genes involved in cell proliferation, apoptosis, and angiogenesis. Intriguingly, we found no evidence that Bmi1 regulates Ink4A/Arf expression in both *in vitro* and *in vivo* systems of liver tumor development. In summary, our study shows that Bmi1 can cooperate with other oncogenic signals to promote hepatic carcinogenesis *in vivo*. Yet Bmi1 functions independent of Ink4A/Arf repression in liver cancer development. (Mol Cancer Res 2009;7(12):1937–45)

Introduction

Bmi1, a member of the mammalian polycomb group of multimeric transcriptional repressors, is involved in the regulation of development, stem cell self-renewal, cell cycle, and senescence (1). Bmi1 was first identified as a c-*myc* cooperating oncogene in murine B-cell lymphomas (2). Subsequent studies have revealed that Bmi1 is required by both normal and leukemic hematopoietic stem cells to maintain their proliferative capacity (3, 4). In addition, Bmi1 has been shown to be important for self-renewal of neural stem cells (5), and its expression is essential for the tumorigenicity of MycN-induced neuroblastoma (6). Studies have found that Bmi1 induces telomerase activity and subsequently immortalizes mammary epithelial cells (7). Perhaps the most prominent link between Bmi1 and tumor development is its inhibition of the *Ink4A/Arf* locus, which results in the regulation of cell senescence and proliferation (8, 9).

Deregulation of Bmi1 expression has been reported in multiple tumor types, including non–small cell lung carcinoma, colon carcinoma, medulloblastoma, metastatic melanoma, and nasopharyngeal carcinoma (10-14). Upregulation of Bmi1 in human hepatocellular carcinoma (HCC) has also been reported (15, 16). In a recent study, Chiba et al. (17) showed that silencing Bmi1 expression decreased the side population (SP) cells in HCC cell lines. These SP subpopulation cells are considered to harbor cancer stem cell like properties (18). However, the exact role of Bmi1 during HCC pathogenesis remains unclear. There are currently no *in vivo* models, which show that Bmi1 functions as an oncogene and directly contributes to HCC pathogenesis.

In this article, we describe that Bmi1 is overexpressed in human HCC samples. Bmi1 expression is also required for HCC cell proliferation *in vitro*. Notably, we established a novel mouse model for Bmi1 and show that Bmi1 can cooperate with activated Ras signaling to promote hepatic carcinogenesis *in vivo*. However, expression analysis suggests that Bmi1 functions independent of its ability to repress Ink4A/Arf tumor suppressor genes. Our data therefore provide solid evidence for a functional role of Bmi1 in liver cancer pathogenesis.

Results

Bmi1 Is Overexpressed in Human HCC Samples

In our previous studies, we used genomic approaches, including cDNA microarray and array-based comparative genomic hybridization, to characterize molecular variations in human HCC (19-21). We identified 703 genes, which are highly expressed in human HCC (21). One of these upregulated genes is *Bmi1*. From this microarray study, Bmi1 expression is upregulated in human HCC compared with nontumor liver tissues ($P = 2 \times 10^{-6}$, after Bonferoni correction; Fig. 1A).

Received 7/27/09; revised 10/22/09; accepted 10/24/09; published OnlineFirst 11/24/09.

Grant support: NIH grants R21CA131625 and R01CA136606 (X. Chen), R01CA094150 (G.P. Dimri), and P30DK026743 to the University of California at San Francisco liver center.

The costs of publication of this article were defrayed in part by the payment of page charges. This article must therefore be hereby marked *advertisement* in accordance with 18 U.S.C. Section 1734 solely to indicate this fact.

Note: Supplementary data for this article are available at Molecular Cancer Research Online (http://mcr.aacrjournals.org/).

C.-R. Xu, S. Lee, and C. Ho contributed equally to this work.

Requests for reprints: Xin Chen, Box 0446, University of California at San Francisco, 513 Parnassus Avenue, San Francisco, CA 94143. Phone: 415-502-6526; Fax: 415-502-4322. E-mail: xin.chen@ucsf.edu

doi:10.1158/1541-7786.MCR-09-0333

To verify this observation, we performed real-time reverse transcription-PCR (RT-PCR) analysis for Bmi1 expression in an independent liver tumor sample set that have not been previously assayed in microarray studies. Again, we observed upregulation of Bmi1 in HCC samples ($P < 0.001$; Fig. 1B). In two recent studies, the overexpression of Bmi1 in human HCC samples was shown at protein levels (15, 16).

Because p16Ink4A and p14Arf have been considered to be major targets of Bmi1 during tumor development, we investigated whether there is any correlation between Bmi1 and Ink4A/Arf expression in human HCC. On the cDNA microarrays, there was one probe corresponding to the COOH-terminal sequences of Ink4A/Arf, which hybridized to both p16Ink4A and p14Arf. Our analysis of this microarray data found no correlation between Bmi1 and total Ink4A/Arf expression ($R = -0.094$; Fig. 1C). We next assayed the expression of Bmi1, p16Ink4A, and p14Arf individually using real-time RT-PCR in 19 human HCC and 4 nontumor liver tissues. Again, we found no correlation between the expression values of Bmi1 and p16Ink4A or p14Arf (Fig. 1D and E).

Altogether, these data show that Bmi1 is upregulated in human HCC, suggesting that Bmi1 may play a role in HCC pathogenesis. However, Bmi1 expression does not seem to be correlated with the expression of Ink4A/Arf tumor suppressor genes in human HCC samples.

Stable shRNA-Mediated Knockdown of Bmi1 Inhibits Cancer Cell Growth In vitro

Our expression analysis suggests a potential role for Bmi1 during liver tumorigenesis. We therefore decided to study the functional significance of Bmi1 in hepatocarcinogenesis. We found that Bmi1 protein is highly expressed in human HCC cell lines (data not shown). To investigate whether Bmi1 is required during liver cancer development, we stably knocked down its expression using lentiviral shRNA in human HCC cell lines. To better study the relationship of Bmi1 expression and genetic alternations in human HCCs, we chose three HCC cell lines (SK-Hep1, Huh7, and Hep3B) with different genetic variations in α-fetoprotein, p53, p16Ink4A, and p14Arf (Supplementary Table S1).

We infected these cells with lentivirus encoding empty vector pLKO.1, a vector with scrambled shRNA (SC/pLKO.1), or vectors against Bmi1, Bmi1/pLKO.1. Because similar results were obtained using pLKO.1 or SC/pLKO.1 as controls (data not shown), only the data with pLKO.1 are shown here. To exclude nonspecific RNAi-mediated effects, we tested two shRNA constructs that target different regions of the Bmi1 sequence (Bmi1/pLKO.1 #1 and Bmi1/pLKO.1 #2). We found that both Bmi1/pLKO.1 vectors efficiently silenced Bmi1 expression in human HCC cell lines, as confirmed by both real-time RT-PCR and Western blotting (Supplementary Fig. S1; Fig. 2A and B). Therefore, only data from the Bmi1/pLKO.1 #1 studies are shown.

We found that despite different genetic backgrounds and Ink4A/Arf status, silencing of Bmi1 inhibits growth of all three HCC cell lines (Supplementary Fig. S1; Fig. 3A). Furthermore, the expression of cell cycle genes, such as *Cdc2, Cdc20*, and *Bub1* (22), are significantly downregulated in Bmi1/pLKO.1-infected HCC cells (Supplementary Fig. S2; Fig. 3B). In addition, bromodeoxyuridine (BrdUrd) labeling revealed a decreased proliferative rate (Supplementary Fig. S3; Fig. 3C), whereas activated caspase 3 assay showed a slight increase in apoptosis when Bmi1 expression is silenced (data not shown). Finally, cell cycle analysis suggests that loss of Bmi1 perturbs cell cycle regulation and leads to G_2-M accumulation (Supplementary Table S2 and Fig. S4; Table 1; Fig. 3D). There is also an increase of sub-G_1 phase cells in Bmi1/pLKO.1-infected cells, providing further support of increased cell apoptosis when Bmi1 expression is inhibited (Supplementary Fig. S4 and Table S2; Fig. 3D).

In summary, the studies support that Bmi1 expression is required for *in vitro* growth of human HCC cell lines.

Loss of Bmi1 Does Not Lead to Significant Increased Expression of p16Ink4A or p14Arf in HCC Cell Lines

One of the major mechanisms of Bmi1-induced tumor development is its function as a potent inhibitor of *CDKN2A* that encodes two major proteins: p16Ink4A and p14Arf (p19Arf in mice; refs. 8, 23). We first determined whether Bmi1 knockdown affects the mRNA expression of *CDKN2A* genes using real-time RT-PCR. SK-Hep1 cells have a deletion of *Ink4A/Arf* locus, whereas Huh7 cells have strong promoter methylation of *p16Ink4A*. Therefore, p16Ink4A expression is virtually undetectable in these two cell lines, regardless of whether Bmi1 is downregulated (Fig. 2A). In addition, the loss of Bmi1 expression in transfected Hep3B cells does not seem to affect the expression of p16Ink4A. Likewise, we found that silencing Bmi1 expression does not lead to upregulation of p14Arf in Huh7 and Hep3B cells, whereas p14Arf expression is absent in SK-Hep1 cells (Fig. 2A). We next assayed p16Ink4A protein expression in these HCC cell lines (Fig. 2B). Consistent with real-time RT-PCR results, p16Ink4A is undetectable in SK-Hep1 and Huh7 cells, whereas there is little change of p16Ink4A protein levels in Bmi1/pLKO.1-infected cell Hep3B cells (Fig. 2B).

In summary, our data showed that Bmi1 is required for HCC cell proliferation; however, the effect of Bmi1 in promoting HCC cell growth is independent of Ink4A/Arf status.

Overexpression of Bmi1 Cooperates with Activated Ras to Induce HCC in Mice

We next determined whether Bmi1 can function as an oncogene by establishing a mouse model. We reasoned that it is unlikely that Bmi1 alone is sufficient to induce liver cancer formation *in vivo*. Therefore, we searched for other signaling pathways that may be able to cooperate with Bmi1 to promote hepatic carcinogenesis. We chose activated Ras as the second signal, based on studies that have shown that Bmi1 is capable of cooperating with activated Ras to transform cells *in vitro* (24, 25). In addition, Ras/mitogen-activated protein kinase (MAPK) signaling is activated in all human HCC samples (26). Therefore, it represents a critical genetic alteration present in human HCC. Furthermore, studies from our and other laboratories have found that activated Ras alone is not sufficient to induce HCC formation in mice (27, 28).

We applied hydrodynamic transfection to stably express Bmi1 (with COOH-terminal V5 tag) and/or an activated form of N-ras (RasV12) into mouse hepatocytes. These animals were

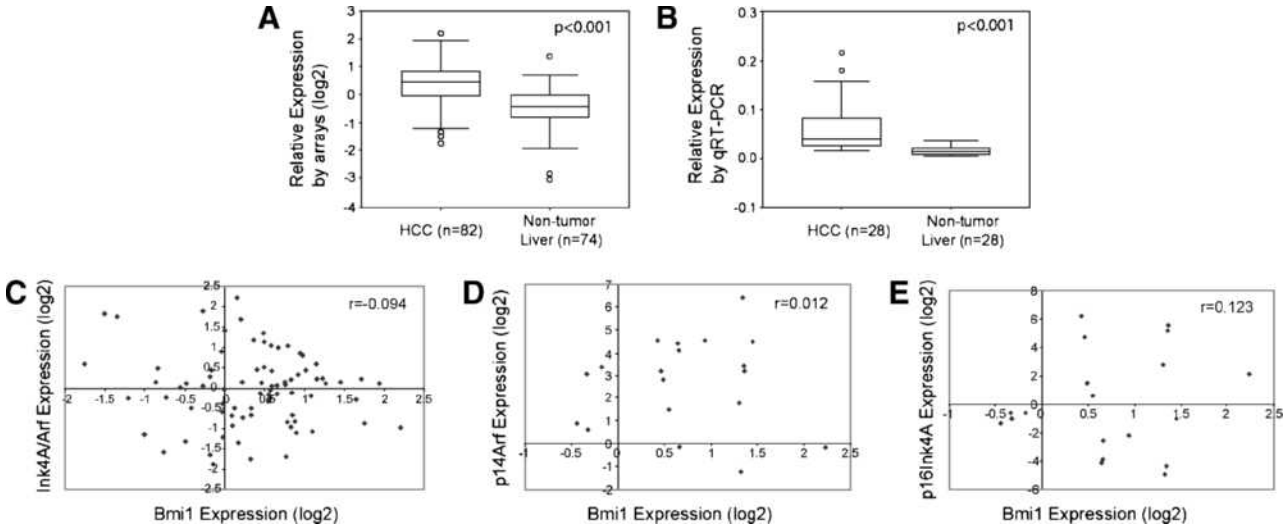

FIGURE 1. Bmi1 expression and its correlation with Ink4A/Arf expression in human HCC samples. **A.** Bmi1 expression in nontumor liver and HCC samples assayed by cDNA microarrays. **B.** Bmi1 expression in an independent liver tissue set assayed by real-time RT-PCR. **C.** Correlation between Bmi1 and Ink4A/Arf expression in human HCC samples assayed by cDNA microarrays. **D** and **E.** Correlation between Bmi1 and p14Arf (**D**) or p16Ink4A (**E**) expression in human HCC samples assayed using real-time RT-PCR.

then monitored and sacrificed at specific time points or when moribund. We found that whereas overexpression of RasV12 ($n = 15$) or Bmi1 ($n = 5$) alone was not sufficient to promote liver tumor development, the coexpression of Bmi1 and RasV12 induced liver tumors in 78.6% (11 of 14) of the mice between 15 and 30 weeks postinjection (Fig. 4A). Tumors tend to be multifocal, sometimes with over 100 tumor nodules scattered around the entire liver (data not shown; Fig. 4B).

Histologic examination of liver tumor samples induced by Bmi1/RasV12 showed that tumors consisted of neoplastic cells with frequent trabecular disorganization, which are characteristic of HCC (Fig. 4D). In most cases, the tumor cells appear to be well differentiated. Real-time RT-PCR analysis revealed high expression of HCC-specific marker α-fetoprotein (Fig. 4C), further confirming the tumors to be of hepatocellular origin.

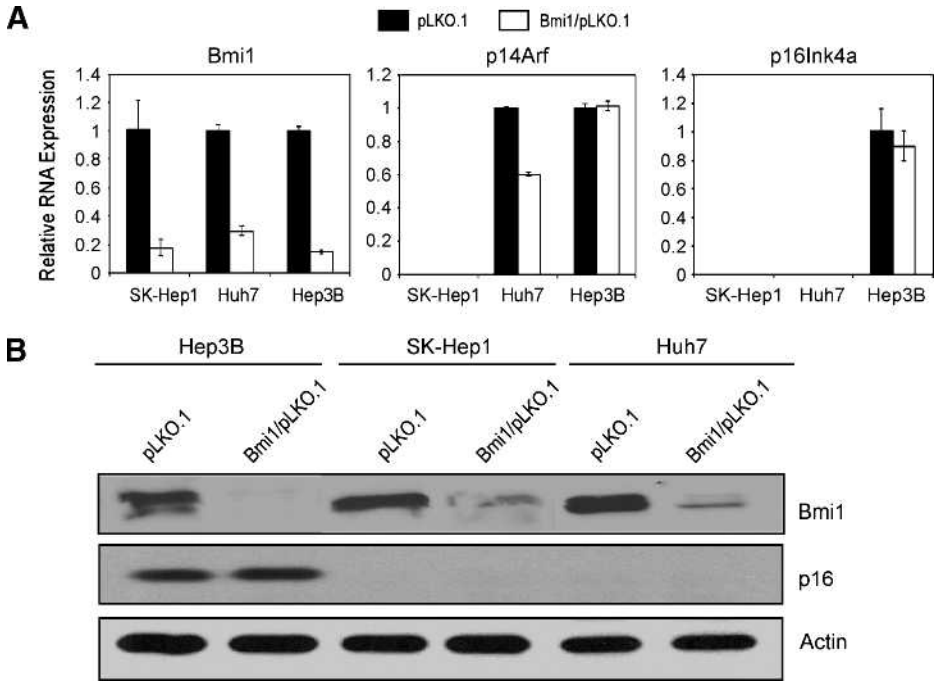

FIGURE 2. Downregulation of Bmi1 and its effects on its target gene expression in human HIC cells. **A.** Real-time RT-PCR analysis of Bmi1, p14Arf, and p16Ink4A in pLKO.1- or Bmi1/pLKO.1-infected HCC cells. **B.** Protein expression of Bmi1 and p16 in pLKO.1- or Bmi1/pLKO.1-infected HCC cells. Actin was used as loading control.

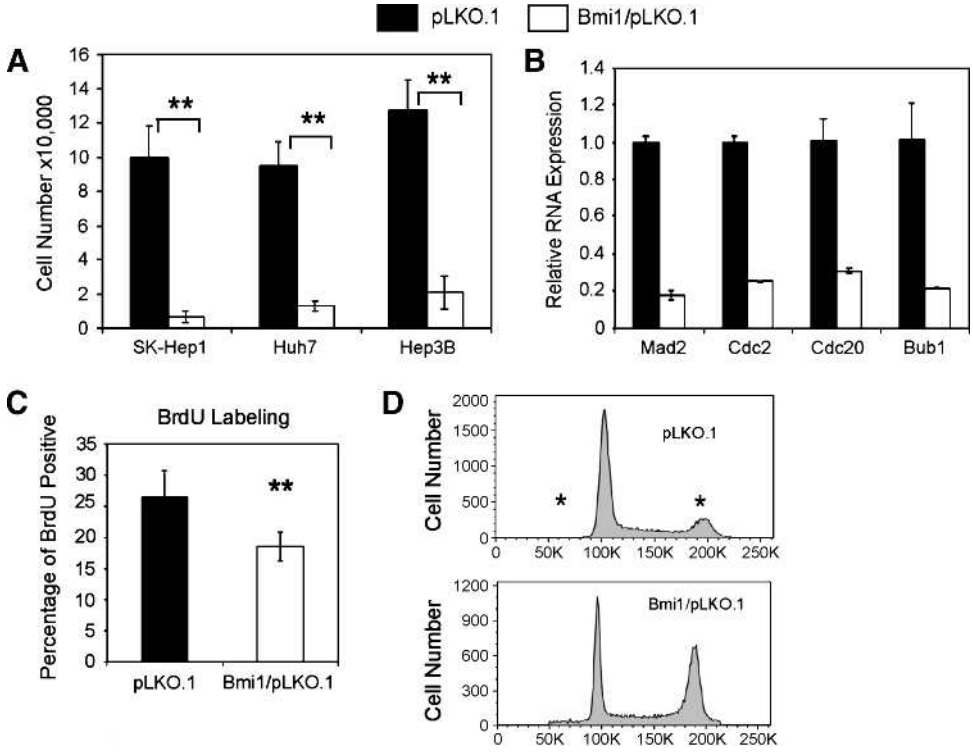

FIGURE 3. Silencing Bmi1 expression leads to decreased cell growth in human HCC cells. **A.** Cell growth assays in three HCC cell lines infected with lentivirus encoding pLKO.1 or Bmi1/pLKO.1. Cell numbers were counted at 3 d postinfection. **B.** Downregulation of cell cycle genes: *Mad2, Cdc2, Cdc20*, and *Bub1* in Bmi1/pLKO.1-infected Huh7 cells. **C.** BrdUrd labeling assay showing a decrease of proliferation in Bmi1/pLKO.1-infected Hep3B cells. **D.** Representative images of cell cycle distribution of Hep3B cells infected with pLKO.1 or Bmi1/pLKO.1 measured by propidium iodide staining and FACS analysis. **, $P < 0.01$; *: $P < 0.05$.

We next examined the tumor nodules for expression of injected Bmi1 (with a COOH-terminal V5 tag) and RasV12. Using anti-V5 antibody, we observed that all tumor cells showed positive nuclear staining of Bmi1 (Fig. 4D). Sporadic expression of Bmi1 was also detected in the hepatocytes of surrounding nontumor liver. RasV12 is indicated by elevated protein levels (Fig. 4E). Because activated Ras is a potent inducer of MAPK signaling, we investigated the activity of RasV12 by assaying for the presence of phospho-ERK. Both Western blot and immunohistochemical analyses detected strong expression of phospho-ERK in the tumors (Fig. 4D and E).

Altogether, these results support that Bmi1 and RasV12 can cooperate to induce HCC *in vivo*.

Molecular Characterization of Bmi1/RasV12 Induced HCC

We then investigated the molecular features of Bmi1/RasV12-induced tumors to determine whether these traits resemble phenotypes observed in human HCC. We first assayed for cell proliferation in Bmi1/RasV12 tumor samples. Our detection of proliferative marker, Ki67, suggested the tumor cells to be highly proliferative (Fig. 5A). We also observed increased expression of cyclin E1 in liver tumor samples, whereas there is little variability in the expression of cell cycle regulator, cyclin D1 (Fig. 5B). In addition, we found that these tumors exhibited elevated levels of cell cycle inhibitor p21 (Fig. 5B), which is likely to be a feedback response to the activated Ras signaling. Furthermore, antiapoptotic marker survivin and cell-cell adhesion marker E-cadherin were also found to be upregulated in liver tumor samples (Fig. 5B). The upregulation of E-cadherin is consistent with well-differentiated tumor histology and is frequently observed in certain mouse models of HCC (29, 30). The occurrence of angiogenesis during liver carcinogenesis can be distinguished by the expression of endothelial markers, like PODXL1 (31). Although PODXL1 is not typically expressed by normal liver sinusoidal endothelial cells, this marker is frequently present in the endothelial cells of liver tumors (31). Therefore, we analyzed our samples for PODXL1 and observed that only endothelial cells within tumor nodules stained positive for this marker (Fig. 5A). Furthermore, these HCC samples also highly expressed angiogenic factor Ang2 (Fig. 5B).

Overall, our data suggests that Bmi1/RasV12-expressing tumors resemble a subset of human HCC characterized by the deregulation of factors involved in proliferation, apoptosis, and angiogenesis.

Table 1. Cell Cycle Distribution: The Percentage of Cells in Each Cell Cycle Phase

	pLKO 1	Bmi1/pLKO 1
Sub-G_1	1.1 ± 2.4	5.1 ± 2.6*
G_1	47.8 ± 2.3	30.7 ± 2.2*
S	34.2 ± 1.3	34.4 ± 2.2
G_2-M	14.6 ± 1.0	27.8 ± 1.7*

*, $P < 0.05$.

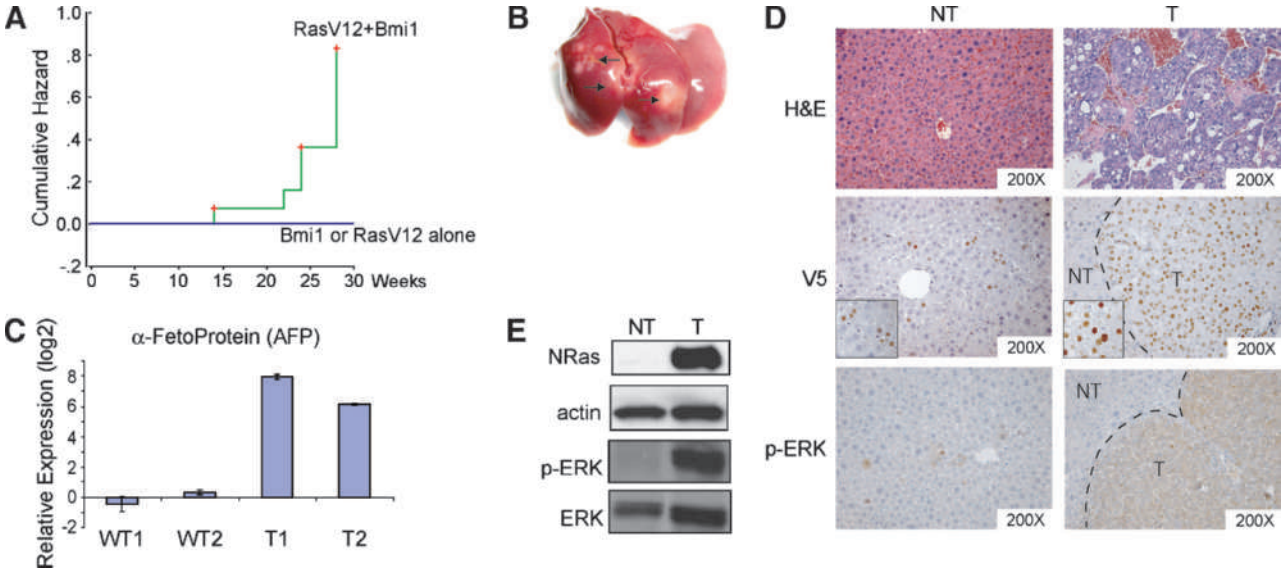

FIGURE 4. Bmi1 cooperates with activated Ras (RasV12) to promote hepatic carcinogenesis *in vivo*. **A.** Tumor development incident curves in mice. The cumulative hazard represents the relative probability of tumor development in each condition. **B.** Representative gross image of liver tumors induced by Bmi1/RasV12. Arrows, visible tumor nodules. **C.** Quantitative RT-PCR analysis of α-fetoprotein expression in normal liver and Bmi1/RasV12 tumor samples. **D.** H&E staining of nontumor liver (*NT*) and HCC (*T*) induced by Bmi1/RasV12 (*top*). Immunohistochemical staining with anti-V5 antibody showing staining of V5-tagged Bmi1 in HCC cells in a tumor nodule, with sporadic staining in nontumor liver tissues (*middle*). Inset, expanded view showing specific nuclear staining of Bmi1 in nontumor liver or HCC cells. Immunohistochemical staining of phospho-ERK in both nontumor liver and HCC samples (*bottom*). **E.** Western blot analysis of N-Ras, phospho-ERK, and ERK expression. Actin was used as loading control.

Upregulation of p16Ink4A/p19Arf Expression in Bmi1/RasV12 Induced Liver Tumors

Bmi1 has been shown to cooperate with RasV12 to transform murine embryonic fibroblast cells via inhibition of *Ink4A/Arf* locus (24). We therefore investigated whether this regulation is a mechanism by which Bmi1 and activated Ras promote tumorigenesis *in vivo*. We examined the expressions of p16Ink4A and p19Arf in our samples by quantitative RT-PCR. We have used multiple primers against p16Ink4A and p19ARF, and we found that in all cases, both p16Ink4A and p19ARF can only be detected after >30 cycles of PCR, indicating that p16Ink4A and p19ARF are expressed at very low levels in normal liver tissues. In contrast, p16Ink4A expression is upregulated ~5-fold and p19Arf expression is upregulated ~50-fold in Bmi1/RasV12 tumor samples (Fig. 6).

Regulation of Ink4A/Arf Expression by RasV12 and Bmi1 in Mouse Hepatocytes

The upregulation of p16Ink4A and p19Arf in Bmi1/RasV12 tumor samples is quite surprising because Bmi1 is a known inhibitor of Ink4A/Arf locus. One of the possibilities is that Ras is a potent inducer of p16Ink4A and p19Arf. The upregulation of Ink4A/Arf may be why activated Ras alone is not sufficient to induce HCC formation *in vivo*. It is possible that the partial inhibition of Ras-induced Ink4A/Arf expression by Bmi1 is what eventually leads to hepatic carcinogenesis. If this is the case, it is likely that Bmi1/RasV12 tumor cells may have somewhat elevated expression of p16Ink4A and p19Arf compared with normal liver. However, this hypothesis is only possible if RasV12 can strongly induce p16Ink4A and p19Arf expression in hepatocytes. We therefore investigated

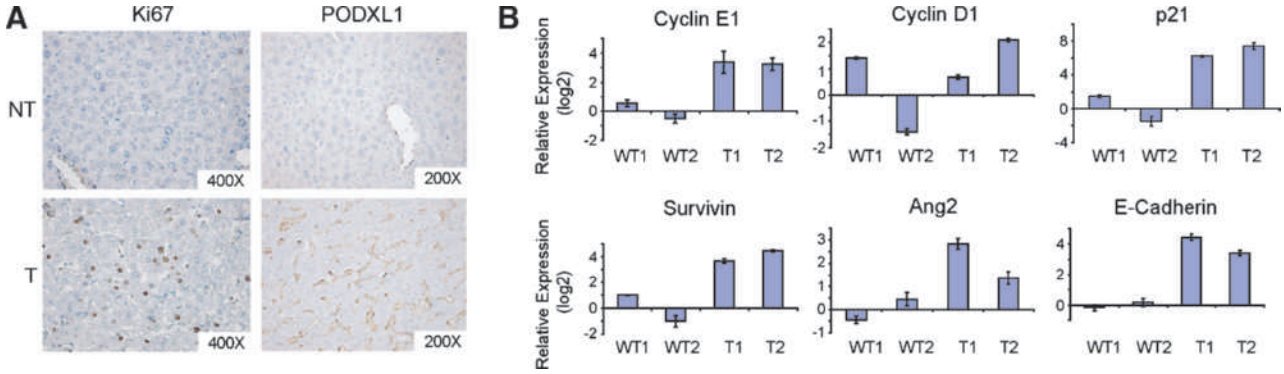

FIGURE 5. Characterization of liver tumors induced by Bmi1/RasV12. **A.** Immunohistochemical staining of Ki67 and PODXL1 in nontumor liver (*NT*) and tumor (*T*) tissues. **B.** Quantitative RT-PCR analysis of genes in two wild-type (*WT*) liver tissues and two Bmi1/Ras liver tumors. In all cases, the expression values of the two wild-type samples were averaged, set to 1, and used to normalize liver tumor samples.

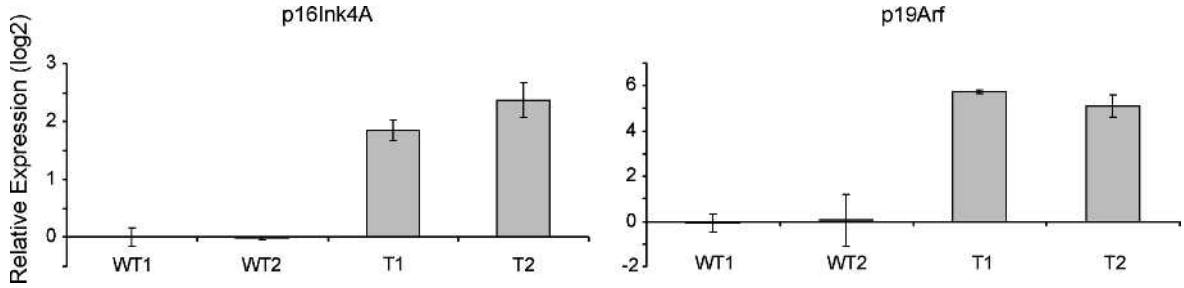

FIGURE 6. Upregulation of p16Ink4A and p19Arf in liver tumor samples induced by Bmi1/RasV12. The relative expression of p16Ink4A and p19Arf of two wild-type liver tissues (WT) and two tumor samples (T) is shown.

the regulation of p16Ink4A and p19Arf by RasV12 or Bmi1 in normal mouse hepatocytes.

First, we generated adenovirus encoding activated Ras. Adenoviral infection has been shown to be able to transfect 100% of mouse hepatocytes at multiplicity of infection of 10 (32). We infected mouse primary hepatocytes with either control adenovirus encoding EGFP (AD-EGFP), or activated Ras (AD-RasV12-HA). Western blot analysis showed the expression of RasV12 in infected cells (Fig. 7A). Using quantitative RT-PCR, we found that p16Ink4A expression is repressed, whereas p19ARF expression remains unchanged in primary mouse hepatocytes after AD-RasV12-HA infection (Fig. 7A). Next, we transfected primary mouse hepatocytes with plasmids encoding activated N-Ras (RasV12-HA) and/or Bmi1 (Bmi1-V5) using Targefect-Hepatocyte transfection reagents, which have a transfection efficiency of 50% for primary hepatocytes. The expression of RasV12 and Bmi1 are indicated by Western blot analysis (Fig. 7B). We found that although the expression of p16Ink4A is downregulated by RasV12 transfection, there is very little change in the expression of p19Arf. Bmi1 upregulates p16Ink4A expression and inhibits p19Arf expression in this condition (Fig. 7B). Cotransfection with Bmi1 and RasV12 showed similar impact on p16Ink4A while having little effect on p19Arf (Fig. 7B). Next, we assayed p16Ink4A protein expression in these mouse hepatocytes. We found that p16Ink4A protein is undetectable in primary mouse hepatocytes in all these conditions (Fig. 7A).

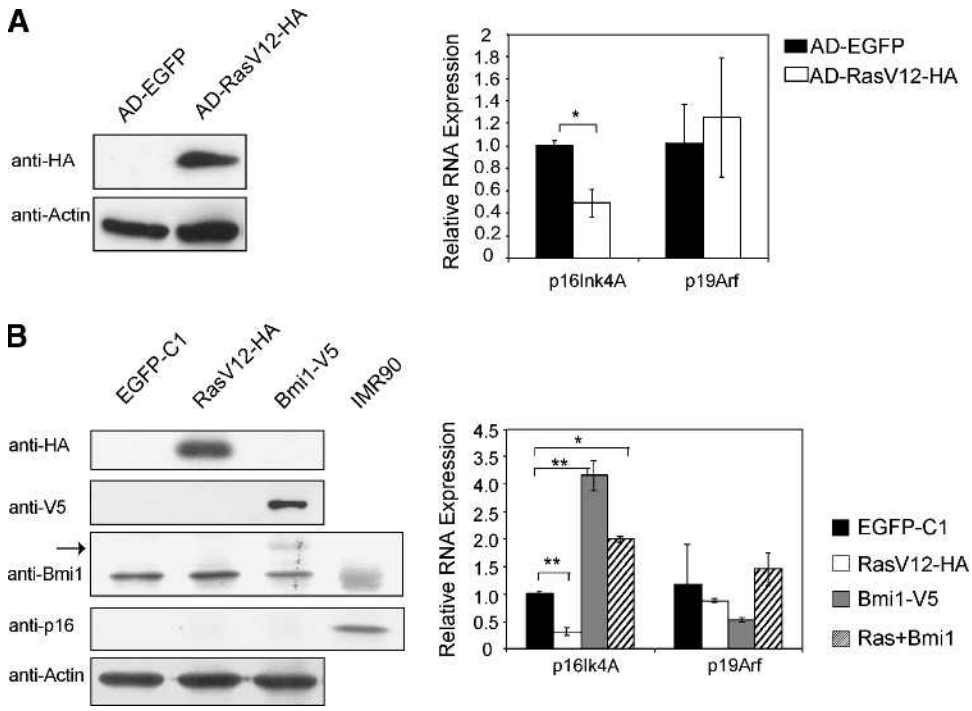

FIGURE 7. Regulation of p16Ink4A and p19Arf expression by RasV12 and/or Bmi1 in primary mouse hepatocytes. **A.** Primary mouse hepatocytes were infected with adenovirus encoding EGFP or RasV12-HA. Western blotting shows the expression of HA-tagged RasV12 (*left*), and real-time RT-PCR shows the quantification of p16Ink4A and p19Arf expression in adenoviral infected primary hepatocytes (*right*). **B.** Primary mouse hepatocytes were transfected with plasmids encoding EGFP, RasV12-HA, and/or Bmi1-V5. Western blotting shows the expression of HA-tagged RasV12, V5-tagged Bmi1, and p16Ink4A (*left*). Arrow, the ectopically expressed Bmi1-V5 that migrates higher than endogenous Bmi1 on gel. IMR90 cell lysate was used as a positive control for p16Ink4A protein expression. Quantification of p16Ink4A and p19Arf mRNA expression in transfected primary hepatocytes was done using real-time RT-PCR (*right*). **, $P < 0.01$; *, $P < 0.05$.

Ras has been shown to induce cell senescence in certain cell types (33, 34), but the induction of cell senescence in hepatocytes by Ras has not been reported. It is possible that Bmi1 cooperates with RasV12 to promote HCC pathogenesis by overcoming Ras-mediated induction of senescence. We therefore investigated whether RasV12 or Bmi1 regulates cell senescence in primary hepatocytes. We transfected primary mouse hepatocytes with EGFP, RasV12, Bmi1, or RasV12 and Bmi1, and assayed for cell senescence. We found no evidence that either RasV12 or Bmi1 can modulate senescent status in primary hepatocytes (Supplementary Fig. S5 Table S3).

In summary, our data do not support activation of Ink4A/Arf by Ras or inhibition of Ink4A/Arf by Bmi1 overexpression in hepatocytes. The experiments therefore indicate that Bmi1 cooperates with RasV12 to promote HCC pathogenesis in an Ink4A/Arf-independent manner.

Discussion

There is increasing evidence supporting Bmi1 as an important oncogene in tumor development. Upregulation of Bmi1 expression has been reported in multiple tumor types. Studies also showed that Bmi1 expression is required for *in vitro* cell proliferation in Ewing Sarcoma, lung cancer, and medulloblastoma cells (35-37), whereas overexpression of Bmi1 enhances cell survival in epidermis (38) and prostate cancer cells (39). Using Bmi1 knockout mice, studies showed that Bmi1 expression is required for the tumorigenesis of leukemia and lung cancer *in vivo* (4, 40). However, there is still little evidence whether Bmi1 overexpression can directly contribute to carcinogenesis, especially in solid tumors. Proper mouse models need to be established to address this critical question. In our current study, we showed that Bmi1 is overexpressed in human HCC samples and required for HCC cell growth *in vitro*. More importantly, we established a novel mouse model that shows that Bmi1 can cooperate with activated Ras to promote HCC pathogenesis in mice. Our study therefore provides pivotal data supporting Bmi1 as an oncogene and its role in hepatic carcinogenesis.

In this study, we used activated Ras to mimic the activation of Ras/MAPK pathway and in combination with Bmi1 to induce HCC in our mouse model. Although there is ubiquitous activation of Ras/MAPK signaling in human HCC, Ras mutations are, in fact, very rare (41, 42). Deregulation of other factors, including tumor suppressor genes *Spry2* and *RASSF1*, overexpression of H-Ras, as well as overactivation of receptor tyrosine kinases, such as epidermal growth factor receptor and c-Met, have been implicated in human HCC, all of which result in upregulation of this pathway (26). Therefore, combination of these genetic alternations with Bmi1 overexpression in mouse models will provide additional *in vivo* models to mimic human HCC pathogenesis. Interestingly, we assayed the expressions of H-Ras and RASSF1A in human HCC samples, and found there to be no correlation between their expressions and Bmi1 expression (Supplementary Fig. S6). Clearly, future experiments will be needed to determine whether the expression of other factors involved in the activation of Ras/MAPK pathways, such as c-Met or epidermal growth factor receptor, are associated with upregulation of Bmi1 expression during HCC pathogenesis.

An important implication of our study is that the tumorigenicity of Bmi1 during HCC pathogenesis is independent of its ability to repress Ink4A/Arf expression. First, we showed there is no correlation between the expressions of Bmi1 and p16Ink4A or p14Arf in human HCC samples. Second, we found that the downregulation of Bmi1 inhibits HCC cell growth independent of Ink4A/Arf status. Finally, we showed that in mouse tumor cells induced by Bmi1/RasV12, there is no downregulation of p16Ink4A or p19Arf expression. Consistent with our observation, several recently published reports have revealed an Ink4A/Arf-independent role for Bmi1 during tumor pathogenesis. Bruggeman et al. (43), for instance, showed that Bmi1 controls mouse glioma development in an Ink4a/Arf-independent manner. Bmi1 knockdown significantly inhibits cell growth in both wild-type and p16Ink4A null Ewing Sarcoma (35), and medulloblastoma cell lines (37). Thus, although inhibition of Ink4A/Arf tumor suppressor gene expression has been widely considered to be the key mechanism of the oncogenic activity of Bmi1, more recent data suggest a critical role of an Ink4A/Arf-independent mechanism for Bmi1 during carcinogenesis.

Clearly, the next step in the characterization of molecular mechanisms of Bmi1 is to identify novel targets and/or pathways regulated by Bmi1 during HCC pathogenesis, and investigate how they cooperate with activated Ras/MAPK signaling to induce liver cancer formation. Some potential targets of Bmi1 have been identified in human cancer cell lines. For example, hTert is thought to be a major target in Bmi1-induced immortalization of mammary epithelial cells (7). *NID1*, a gene related to cell adhesion, has been implicated as a Bmi1 target in Ewing Sarcoma cells (35). Signaling molecules including BMP5, transforming growth factor β2, and Notch2 have been found to be regulated by Bmi1 in medulloblastoma cell lines (37). It would be of interest to determine whether the expression of these factors is modulated by Bmi1 during HCC pathogenesis. A recent study indicated that the loss of Bmi1 results in the increase of reactive oxygen species and subsequent stimulation of the DNA damage response pathway (44). Activation of the DNA damage response pathway has been found to be an important barrier to tumorigenesis. In our recent studies, we observed upregulation in the mRNA of p53 and ATM genes in Bmi1/RasV12-induced liver tumor samples.[8] Clearly, it would be important to further characterize the expression of these genes in tumor samples at protein levels. Analysis of the regulation of this pathway by Bmi1 in liver may identify an additional function for Bmi1 during the development of HCC.

Materials and Methods

Human Tissue Samples and RNA Preparation

Samples of tumor and nontumor liver tissues were collected from liver resections at The University of Hong Kong. Tissues were frozen in liquid nitrogen within 0.5 hour after they were resected. Total RNA was extracted using Trizol (Invitrogen). This study was approved by the Ethics Committee of the University of Hong Kong and the Internal Review Boards from University of California at San Francisco.

[8] S.A. Lee and X. Chen, unpublished observation.

Constructs and Reagents

Two shRNA constructs targeting Bmi1, Bmi1/pLKO.1 #1 (TRCN0000020155, NM_005180.5-693s1c1) and Bmi1/pLKO.1 #2 (TRCN0000020156, NM_005180.5-1061s1c1), used to silence Bmi1 expression were obtained from OpenBiosystems. Control pLKO.1 (empty vector) or SC/PLKO.1 (with a scrambled sequence) plasmids were obtained from Addgene. The hyperactive sleeping beauty construct (pCMV/SB) was provided by Dr. Mark Kay of Stanford University, Stanford, CA, and the pCaggs-RasV12 was provided by Dr. David Largaespada of University of Minnesota, Minneapolis, MN. The pT3-EF1α vector containing duplicated inverted repeats for sleeping beauty–mediated integration and EF1α promoter (pT3-EF1α) used for hydrodynamic injection was described by Tward A et al. (45). Human Bmi1 (with a COOH-terminal V5 tag) was cloned into pT3-EF1α via the Gateway PCR cloning strategy (Invitrogen). All plasmids were purified using the Endotoxin free Maxi prep kit (Sigma) before injecting into mice.

Cell Culture, Lentiviral Infection, Cell Proliferation, BrdUrd Labeling, Caspase-3 Activity, and Cell Cycle Assays

All human HCC cell lines were purchased from American Type Culture Collection except Huh7, which were kindly provided by Dr. Ben Yen of University of California at San Francisco, San Francisco, CA. The cells are cultured in DMEM plus 10% fetal bovine serum. Lentivirus was generated and used to infect HCC cells. Three days postinfection, cells were expanded and selected with 1 μg/mL puromycin for 3 d and harvested for protein or RNA analysis. To assay cell proliferation rate, equal number of cells were seeded in six-well plates and counted 3 to 4 d postseeding. Cell cycle analysis was done by flow cytometry after propidium iodide staining, and the results were analyzed using FlowJo. BrdUrd labeling was as described (46) and Caspase-3 activity was measured using Caspase-Glo3/7 Assay kit (Promega).

Hepatocyte Isolation, Transfection, Adenovirus Infection, and Cell Senescence Assay

Primary hepatocyte isolation was done using standard collagenase perfusion method as described (47). The hepatocytes were transfected with plasmids using Targefect-Hepatocyte reagents (Targeting Systems) per manufacturer's instruction. Ad-H-RasV12 was kindly provided by Dr. Judy Meinkoth of the University of Pennsylvania, Philadelphia, PA (48). Adenovirus was amplified and titered by Vector Biolabs and used to infect primary hepatocytes at 50 multiplicity of infection. Hepatocytes were harvested 30 h posttransfection or infection. Hepatocyte senescence was determined using senescence β-galactosidase staining kit (Cell Signaling Technology).

Mouse Hydrodynamic Transfection and Monitoring

Wild-type FVB/N mice were used in this study. The hydrodynamic transfection procedure are as described previously (45). The injected mice were monitored weekly and sacrificed between 14 to 30 wk postinjection. All mice were housed, fed, and treated in accordance with protocols approved by the committee for animal research at the University of California at San Francisco.

Histology and Immunohistochemistry

Animals were euthanized and their livers were removed and rinsed in PBS. Samples collected from the livers were either frozen in dry ice for RNA and protein extraction or fixed overnight in freshly prepared cold 4% paraformaldehyde. Fixed tissue samples were embedded in paraffin. Five-micron sections were placed on slides and stained with H&E. Immunohistochemistry was done as described (28). Antibodies and dilutions were as follows: anti-V5, 1:1000 (Invitrogen); anti–phospho-ERK, 1:100 (Cell Signaling Technology); anti-PODXL1, 1:200 (Applied Genomics); and anti-Ki67, 1:150 (Lab vision).

Preparation of Lysates and Western Blotting

Liver tissues or cell lines were lysed in M-PER mammalian protein extraction buffer (Pierce) plus proteinase inhibitor cocktail (Roche) and Halt phosphotase inhibitor cocktail (Pierce). Protein content of the lysate was quantified using the BCA protein assay (Pierce). Western blotting was done as described (45). Antibodies were used as follows: anti-Bmi1, 1:1,000 (Millipore) or 1:1,000 (Invitrogen); anti–phospho-ERK, 1:1,000; anti-ERK, 1:1,000 (Cell Signaling Technology); anti-actin, 1:1,000 (Sigma); anti-V5, 1:5,000 (Invitrogen); anti-NRas, 1:1,000; anti-p16, 1:1,000; and anti-HA, 1:1,000 (Santa Cruz Biotechnology).

Real-time RT-PCR

Total RNA was extracted from frozen liver tissues using Trizol (Invitrogen) and digested with DNase I to remove any genomic DNA contamination. Sybergreen-based real-time RT-PCR was carried out as described (21), and rRNA was used as internal control. Transcript quantification was done in triplicate for every sample and reported relative to rRNA. The primer pairs used are listed in Supplementary Table S4.

Statistical Analysis

The Pearson's correlation coefficient (R) was used to determine the correlations between gene expression values, and P value was determined using SPSS statistical program. Student's t test was used to evaluate statistical significance among experimental groups. Values of $P < 0.05$ were considered to be significant.

Disclosure of Potential Conflicts of Interest

No potential conflicts of interest are disclosed.

Acknowledgments

We thank Sandra Huling of the University of California, San Francisco Liver Center Morphology Core for histology support; Ali Naqvi, Theresa Canavan, and Chris Her of the Cell and Tissue Biology Core for isolating mouse hepatocytes; Ali Brincat and Xiaoyin Wang of Sandler Lentivirus Core for lentivirus production; Bill Hyun for fluorescence-activated cell sorting analysis; and Drs. David Largaespada, Mark Kay, Judy Meinkoth, and Ben Yen for reagents used in the study.

References

1. Valk-Lingbeek ME, Bruggeman SW, van Lohuizen M. Stem cells and cancer; the polycomb connection. Cell 2004;118:409–18.

2. Haupt Y, Alexander WS, Barri G, Klinken SP, Adams JM. Novel zinc finger gene implicated as myc collaborator by retrovirally accelerated lymphomagenesis in E mu-myc transgenic mice. Cell 1991;65:753–63.

3. Park IK, Qian D, Kiel M, et al. Bmi-1 is required for maintenance of adult self-renewing haematopoietic stem cells. Nature 2003;423:302–5.

4. Lessard J, Sauvageau G. Bmi-1 determines the proliferative capacity of normal and leukaemic stem cells. Nature 2003;423:255–60.

5. Molofsky AV, Pardal R, Iwashita T, Park IK, Clarke MF, Morrison SJ. Bmi-1 dependence distinguishes neural stem cell self-renewal from progenitor proliferation. Nature 2003;425:962–7.

6. Cui H, Hu B, Li T, et al. Bmi-1 is essential for the tumorigenicity of neuroblastoma cells. Am J Pathol 2007;170:1370–8.

7. Dimri GP, Martinez JL, Jacobs JJ, et al. The Bmi-1 oncogene induces telomerase activity and immortalizes human mammary epithelial cells. Cancer Res 2002; 62:4736–45.

8. Park IK, Morrison SJ, Clarke MF. Bmi1, stem cells, and senescence regulation. J Clin Invest 2004;113:175–9.

9. Lobo NA, Shimono Y, Qian D, Clarke MF. The biology of cancer stem cells. Annu Rev Cell Dev Biol 2007;23:675–99.

10. Leung C, Lingbeek M, Shakhova O, et al. Bmi1 is essential for cerebellar development and is overexpressed in human medulloblastomas. Nature 2004;428: 337–41.

11. Vonlanthen S, Heighway J, Altermatt HJ, et al. The bmi-1 oncoprotein is differentially expressed in non-small cell lung cancer and correlates with INK4A-ARF locus expression. Br J Cancer 2001;84:1372–6.

12. Kim JH, Yoon SY, Kim CN, et al. The Bmi-1 oncoprotein is overexpressed in human colorectal cancer and correlates with the reduced p16INK4a/p14ARF proteins. Cancer Lett 2004;203:217–24.

13. Mihic-Probst D, Kuster A, Kilgus S, et al. Consistent expression of the stem cell renewal factor BMI-1 in primary and metastatic melanoma. Int J Cancer 2007;121:1764–70.

14. Sacchi S, Federico M, Dastoli G, et al. Treatment of B-cell non-Hodgkin's lymphoma with anti CD 20 monoclonal antibody Rituximab. Crit Rev Oncol Hematol 2001;37:13–25.

15. Wang H, Pan K, Zhang HK, et al. Increased polycomb-group oncogene Bmi-1 expression correlates with poor prognosis in hepatocellular carcinoma. J Cancer Res Clin Oncol 2008;134:535–41.

16. Sasaki M, Ikeda H, Itatsu K, et al. The overexpression of polycomb group proteins Bmi1 and EZH2 is associated with the progression and aggressive biological behavior of hepatocellular carcinoma. Lab Invest 2008.

17. Chiba T, Miyagi S, Saraya A, et al. The polycomb gene product BMI1 contributes to the maintenance of tumor-initiating side population cells in hepatocellular carcinoma. Cancer Res 2008;68:7742–9.

18. Chiba T, Kita K, Zheng YW, et al. Side population purified from hepatocellular carcinoma cells harbors cancer stem cell-like properties. Hepatology 2006; 44:240–51.

19. Chen X, Cheung ST, So S, et al. Gene expression patterns in human liver cancers. Mol Biol Cell 2002;13:1929–39.

20. Patil MA, Gutgemann I, Zhang J, et al. Array-based comparative genomic hybridization reveals recurrent chromosomal aberrations and Jab1 as a potential target for 8q gain in hepatocellular carcinoma. Carcinogenesis 2005;26:2050–7.

21. Patil MA, Chua MS, Pan KH, et al. An integrated data analysis approach to characterize genes highly expressed in hepatocellular carcinoma. Oncogene 2005; 24:3737–47.

22. Whitfield ML, Sherlock G, Saldanha AJ, et al. Identification of genes periodically expressed in the human cell cycle and their expression in tumors. Mol Biol Cell 2002;13:1977–2000.

23. Pardal R, Molofsky AV, He S, Morrison SJ. Stem cell self-renewal and cancer cell proliferation are regulated by common networks that balance the activation of proto-oncogenes and tumor suppressors. Cold Spring Harbor Symp Quant Biol 2005;70:177–85.

24. Jacobs JJ, Kieboom K, Marino S, DePinho RA, van Lohuizen M. The oncogene and Polycomb-group gene bmi-1 regulates cell proliferation and senescence through the ink4a locus. Nature 1999;397:164–8.

25. Datta S, Hoenerhoff MJ, Bommi P, et al. Bmi-1 cooperates with H-Ras to transform human mammary epithelial cells via dysregulation of multiple growth-regulatory pathways. Cancer Res 2007;67:10286–95.

26. Calvisi DF, Ladu S, Gorden A, et al. Ubiquitous activation of Ras and Jak/Stat pathways in human HCC. Gastroenterology 2006;130:1117–28.

27. Harada N, Oshima H, Katoh M, Tamai Y, Oshima M, Taketo MM. Hepatocarcinogenesis in mice with β-catenin and Ha-ras gene mutations. Cancer Res 2004;64:48–54.

28. Lee SA, Ho C, Roy R, et al. Integration of genomic analysis and *in vivo* transfection to identify sprouty 2 as a candidate tumor suppressor in liver cancer. Hepatology 2008;47:1200–10.

29. Calvisi DF, Ladu S, Conner EA, Factor VM, Thorgeirsson SS. Disregulation of E-cadherin in transgenic mouse models of liver cancer. Lab Invest 2004;84: 1137–47.

30. Wei Y, Van Nhieu JT, Prigent S, Srivatanakul P, Tiollais P, Buendia MA. Altered expression of E-cadherin in hepatocellular carcinoma: correlations with genetic alterations, β-catenin expression, and clinical features. Hepatology 2002; 36:692–701.

31. Chen X, Higgins J, Cheung ST, et al. Novel endothelial cell markers in hepatocellular carcinoma. Mod Pathol 2004.

32. Prost S, Sheahan S, Rannie D, Harrison DJ. Adenovirus-mediated Cre deletion of floxed sequences in primary mouse cells is an efficient alternative for studies of gene deletion. Nucleic Acids Res 2001;29:E80.

33. Serrano M, Lin AW, McCurrach ME, Beach D, Lowe SW. Oncogenic ras provokes premature cell senescence associated with accumulation of p53 and p16INK4a. Cell 1997;88:593–602.

34. Lin AW, Barradas M, Stone JC, van Aelst L, Serrano M, Lowe SW. Premature senescence involving p53 and p16 is activated in response to constitutive MEK/MAPK mitogenic signaling. Genes Dev 1998;12:3008–19.

35. Douglas D, Hsu JH, Hung L, et al. BMI-1 promotes ewing sarcoma tumorigenicity independent of CDKN2A repression. Cancer Res 2008;68:6507–15.

36. Yu Q, Su B, Liu D, et al. Antisense RNA-mediated suppression of Bmi-1 gene expression inhibits the proliferation of lung cancer cell line A549. Oligonucleotides 2007;17:327–35.

37. Wiederschain D, Chen L, Johnson B, et al. Contribution of polycomb homologues Bmi-1 and Mel-18 to medulloblastoma pathogenesis. Mol Cell Biol 2007; 27:4968–79.

38. Lee K, Adhikary G, Balasubramanian S, et al. Expression of Bmi-1 in epidermis enhances cell survival by altering cell cycle regulatory protein expression and inhibiting apoptosis. J Invest Dermatol 2008;128:9–17.

39. Fan C, He L, Kapoor A, et al. Bmi1 promotes prostate tumorigenesis via inhibiting p16(INK4A) and p14(ARF) expression. Biochim Biophys Acta 2008;1782:642–8.

40. Dovey JS, Zacharek SJ, Kim CF, Lees JA. Bmi1 is critical for lung tumorigenesis and bronchioalveolar stem cell expansion. Proc Natl Acad Sci U S A 2008;105:11857–62.

41. Tsuda H, Hirohashi S, Shimosato Y, Ino Y, Yoshida T, Terada M. Low incidence of point mutation of c-Ki-ras and N-ras oncogenes in human hepatocellular carcinoma. Jpn J Cancer Res 1989;80:196–9.

42. Challen C, Guo K, Collier JD, Cavanagh D, Bassendine MF. Infrequent point mutations in codons 12 and 61 of ras oncogenes in human hepatocellular carcinomas. J Hepatol 1992;14:342–6.

43. Bruggeman SW, Hulsman D, Tanger E, et al. Bmi1 controls tumor development in an Ink4a/Arf-independent manner in a mouse model for glioma. Cancer Cell 2007;12:328–41.

44. Liu J, Cao L, Chen J, et al. Bmi1 regulates mitochondrial function and the DNA damage response pathway. Nature 2009.

45. Tward AD, Jones KD, Yant S, et al. Distinct pathways of genomic progression to benign and malignant tumors of the liver. Proc Natl Acad Sci U S A 2007.

46. Wojtowicz JM, Kee N. BrdU assay for neurogenesis in rodents. Nat Protoc 2006;1:1399–405.

47. Nelsen CJ, Rickheim DG, Tucker MM, Hansen LK, Albrecht JH. Evidence that cyclin D1 mediates both growth and proliferation downstream of TOR in hepatocytes. J Biol Chem 2003;278:3656–63.

48. Cheng G, Lewis AE, Meinkoth JL. Ras stimulates aberrant cell cycle progression and apoptosis in rat thyroid cells. Mol Endocrinol 2003;17:450–9.